



**Development of the  
high-order decoupled  
direct method**

W. Zhang et al.

This discussion paper is/has been under review for the journal Geoscientific Model Development (GMD). Please refer to the corresponding final paper in GMD if available.

# Development of the high-order decoupled direct method in three dimensions for particulate matter: enabling advanced sensitivity analysis in air quality models

W. Zhang<sup>1</sup>, S. L. Capps<sup>2</sup>, Y. Hu<sup>3</sup>, A. Nenes<sup>1,2</sup>, S. L. Napelenok<sup>4</sup>, and A. G. Russell<sup>3</sup>

<sup>1</sup>School of Earth and Atmospheric Sciences, Georgia Institute of Technology, Atlanta, Georgia, USA

<sup>2</sup>School of Chemical and Biomolecular Engineering, Georgia Institute of Technology, Atlanta, Georgia, USA

<sup>3</sup>School of Civil and Environmental Engineering, Georgia Institute of Technology, Atlanta, Georgia, USA

<sup>4</sup>US Environment Protection Agency, Research Triangle Park, North Carolina, USA

Received: 5 August 2011 – Accepted: 14 September 2011 – Published: 4 October 2011

Correspondence to: W. Zhang (wxzhang@gatech.edu)

Published by Copernicus Publications on behalf of the European Geosciences Union.

Title Page

Abstract

Introduction

Conclusions

References

Tables

Figures



Back

Close

Full Screen / Esc

Printer-friendly Version

Interactive Discussion



## Abstract

The high-order decoupled direct method in three dimensions for particulate matter (HDDM-3D/PM) has been implemented in the Community Multiscale Air Quality (CMAQ) model to enable advanced sensitivity analysis. The major effort of this work is to develop high-order DDM sensitivity analysis of ISORROPIA, the inorganic aerosol module of CMAQ. A case-specific approach has been applied, and the sensitivities of activity coefficients and water content are explicitly computed. Stand-alone tests are performed for ISORROPIA by comparing the sensitivities (first- and second-order) computed by HDDM and the brute force (BF) approximations. Similar comparison has also been carried out for CMAQ results simulated using a week-long winter episode for a continental US domain. Second-order sensitivities of aerosol species (e.g., sulfate, nitrate, and ammonium) with respect to domain-wide  $\text{SO}_2$ ,  $\text{NO}_x$ , and  $\text{NH}_3$  emissions show agreement with BF results, yet exhibit less noise in locations where BF results are demonstrably inaccurate. Second-order sensitivity analysis elucidates nonlinear responses of secondary inorganic aerosols to their precursors and competing species that have not yet been well-understood with other approaches. Including second-order sensitivity coefficients in the Taylor series projection of the nitrate concentrations with a 50% reduction in domain-wide  $\text{NO}_x$  emission shows a statistically significant improvement compared to the first-order Taylor series projection.

## 1 Introduction

Airborne particulate matter (PM), or aerosol, is a major pollutant in the atmosphere. Studies have shown that PM impairs visibility (Watson, 2002), may cause harmful effects on ecosystems (Galloway et al., 2004), and affects human health (e.g., Zanobetti et al., 2000; Kaiser, 2005). In response, control strategies are designed to lower the concentrations of anthropogenic PM in the atmosphere (US EPA, 2004). Historically, multiple air quality model simulations using different sets of emissions have been used

# GMDD

4, 2605–2633, 2011

## Development of the high-order decoupled direct method

W. Zhang et al.

[Title Page](#)

[Abstract](#)

[Introduction](#)

[Conclusions](#)

[References](#)

[Tables](#)

[Figures](#)



[Back](#)

[Close](#)

[Full Screen / Esc](#)

[Printer-friendly Version](#)

[Interactive Discussion](#)



to evaluate the expected benefit of different strategies (e.g., Bergin et al., 2008). This approach is resource-intensive (Dunker, 1984), and the numerical precision of models limits the size of emissions changes that can be actually evaluated (Hakami et al., 2004). An alternative approach is to use sensitivity analysis tools integrated in the simulation.

Sensitivity analysis reveals the relationship of model outputs (e.g., pollutant concentrations) to model input parameters (e.g., emissions rates, initial or boundary conditions, and chemical reaction rates). Quantitatively, they express partial derivatives as the “sensitivity coefficients”, and are calculated by several methods. One approach is the brute force (BF) approximation; using central finite difference approximation, first- and second-order sensitivities are expressed as:

$$S_{ij}^{(1),BF} = \frac{C_i|_{p_j+\Delta p_j} - C_i|_{p_j-\Delta p_j}}{2\Delta p_j} \quad (1)$$

$$S_{ijj}^{(2),BF} = \frac{C_i|_{p_j+\Delta p_j} - 2C_i|_{p_j} + C_i|_{p_j-\Delta p_j}}{(\Delta p_j)^2} \quad (2)$$

where  $S_{ij}^{(1),BF}$  and  $S_{ijj}^{(2),BF}$  represent the brute force first-order and second-order sensitivities, respectively of species  $i$  with respect to parameter  $p_j$  (e.g., emissions, initial or boundary conditions, or reaction rates).  $C_i$  represents the concentration of species  $i$ . The subscripts indicate the locations where the concentrations are evaluated. Computational requirements for BF sensitivity analysis scale with the number of parameters investigated. Obviously, BF becomes resource-intensive with an increasing number of parameters of interest or with increasing order (e.g., second order or higher) of sensitivities. In addition to being computationally inefficient, the BF sensitivities are prone to considerable numerical noise. One reason for the numerical noise is the truncation errors, which are introduced by omitting the higher-order terms when deriving Eqs. (1) and (2) from Taylor series expansion. The truncation error is a function of both the perturbation ( $\Delta p$ ) and the higher-order sensitivities. If the system is highly nonlinear, even

## GMDD

4, 2605–2633, 2011

### Development of the high-order decoupled direct method

W. Zhang et al.

Title Page

Abstract

Introduction

Conclusions

References

Tables

Figures



Back

Close

Full Screen / Esc

Printer-friendly Version

Interactive Discussion



a small perturbation can cause sizable truncation error (Hakami et al., 2004). Another reason for the numerical noises of BF is due to the modeling accuracy and precision. For example, incomplete convergence in iterative solvers will cause such errors. Both types of errors for second-order BF sensitivities are amplified compared to first-order BF sensitivities. Actually, as the order of sensitivities increase, BF approximations become significantly less accurate (Hakami et al., 2004).

An alternative approach to BF is the decoupled direct method in three dimensions (DDM-3D). This method operates integrally within a chemical transport model (CTM) and simultaneously computes local sensitivities of pollutant concentrations to perturbations in input parameters (Dunker, 1984; Yang et al., 1997; Cohan et al., 2005; Napelenok et al., 2006; Cohan et al., 2010). DDM-3D sensitivities are calculated by solving sensitivity equations that are the derivatives of the partial differential equations governing the CTM. DDM-3D is computationally efficient for large number of sensitivity parameters and is subject to considerably less numerical noise. DDM-3D has been implemented in CTMs (e.g., CMAQ; Byun and Schere, 2006, CAMx; ENVIRON, 2005) to conduct source impact analysis for ozone and PM (Yang et al., 1997; Mendoza-Dominguez and Russell, 2000; Odman et al., 2002; Napelenok et al., 2006; Koo et al., 2007). Initially, DDM-3D was applied to calculate first-order sensitivities, which are the locally linear responses of pollutant concentrations to changes in model inputs and parameters (e.g., emissions, and initial and boundary conditions) at the conditions currently modeled.

DDM-3D has been extended to calculate high-order sensitivities of gaseous species by Hakami et al. (2003) within the Multiscale Air Quality Simulation Platform (MAQSIP) (Odman and Ingram, 1996). They calculated second- and third-order sensitivities using DDM-3D and showed that the approach could accurately capture the nonlinear response of ozone concentration to  $\text{NO}_x$  and VOC emission changes. They also investigated the efficiency of DDM-3D in calculating high-order sensitivities. An important outcome of that work was that higher than second order sensitivities are not necessary for the majority of potential applications. More recently, the high-order approach for

## GMDD

4, 2605–2633, 2011

### Development of the high-order decoupled direct method

W. Zhang et al.

[Title Page](#)

[Abstract](#)

[Introduction](#)

[Conclusions](#)

[References](#)

[Tables](#)

[Figures](#)



[Back](#)

[Close](#)

[Full Screen / Esc](#)

[Printer-friendly Version](#)

[Interactive Discussion](#)



## Development of the high-order decoupled direct method

W. Zhang et al.

Title Page

Abstract

Introduction

Conclusions

References

Tables

Figures

⏪

⏩

◀

▶

Back

Close

Full Screen / Esc

Printer-friendly Version

Interactive Discussion



gaseous species has also been implemented in the Community Multiscale Air Quality (CMAQ) model (Cohan et al., 2005) and the Comprehensive Air Quality with extensions (CAMx) (Koo et al., 2010). High-order sensitivity calculations of gaseous species have been applied to source apportionment and air quality model uncertainty analysis (Cohan et al., 2005; Tian et al., 2010). Although nonlinear effects of aerosol precursors on aerosol concentrations have been of concern in the past decade (Ansari and Pandis, 1998; West and Pandis, 1999), developing HDDM for PM has not yet been undertaken due to the discontinuous, highly nonlinear solution surface of the inorganic aerosol thermodynamics. Only now has the challenging task of extending high-order, direct sensitivity analysis to particulate matter species been accomplished. HDDM-3D/PM is implemented in the Community Multidimensional Air Quality model, version 4.5 (CMAQ4.5).

## 2 Model description

CMAQ is an Eulerian air quality model (Byun and Schere, 2006) that simulates emissions, deposition, transport and chemical transformation of atmospheric species primarily by solving the advection-diffusion-reaction equations:

$$\frac{\partial C_i}{\partial t} = -\nabla(\mathbf{u}C_i) + \nabla(\mathbf{K}\nabla C_i) + R_i + E_i \quad (3)$$

where  $C_i$  is the concentration of the  $i$ -th species,  $\mathbf{u}$  the fluid velocity,  $\mathbf{K}$  the turbulence diffusivity,  $R_i$  the chemical reaction rate of the  $i$ -th species, and  $E_i$  the emission rate for the  $i$ -th species (Seinfeld and Pandis, 2006). The chemicals species can be in gas phase or aerosol form.

In the modal treatment of aerosol in CMAQ, aerosol species are tracked based on their size using three modes: Aitken, accumulation, and coarse. The two smaller modes (noted as Aitken and accumulation modes, respectively) approximately represent  $\text{PM}_{2.5}$ , aerosols smaller than  $2.5 \mu\text{m}$  in aerodynamic diameter. CMAQ includes

---

**Development of the high-order decoupled direct method**W. Zhang et al.

---

[Title Page](#)[Abstract](#)[Introduction](#)[Conclusions](#)[References](#)[Tables](#)[Figures](#)[Back](#)[Close](#)[Full Screen / Esc](#)[Printer-friendly Version](#)[Interactive Discussion](#)

modeled processes of secondary inorganic aerosol (i.e., sulfate, nitrate, ammonium), anthropogenic secondary organic aerosol (SOA), and biogenic SOA formation as well as primary emissions of elemental carbon and sea salt in the Aitken and accumulation modes.  $PM_{2.5}$  changes in response to new particle production from vapor phase precursors, coagulation of particles, growth by condensation from gaseous species, transport and deposition of particles, and emissions (Byun and Schere, 2006). The concentration of  $PM_{2.5}$  is highly dependent on gas phase species concentrations because of the significant fraction of secondary aerosol in this size range. CMAQ4.5 assumes the secondary inorganic aerosols are in thermodynamic equilibrium with surrounding gases, and uses ISORROPIAv1.7 (Nenes et al., 1998a; Fountoukis et al., 2007) to simulate their condensation and evaporation. This approach has also been used by CMAQ4.7 to simulate the chemical interactions between coarse particles and gas-phase pollutants (Kelly et al., 2010). CMAQ4.5 partitions SOA between gas and condensed phase based on the two-product model of Odum et al. (1997) using empirically derived coefficients from chamber experiments (Schell et al., 2001). The algorithm to compute SOA concentrations is similar to that of photochemical reactions.

ISORROPIA assumes that equilibrium exists between gas phases and aerosol species and uses thermodynamics to calculate the composition of inorganic aerosols and concentrations of surrounding gases. Inputs to ISORROPIA include the total (gas and aerosol) concentrations of five inorganic precursor species (i.e., sulfate, nitrate, ammonium, sodium, and chloride), temperature, and relative humidity. To determine the aerosol composition at equilibrium, ISORROPIA first identifies the solution regime of the given system based on sulfate ratio (i.e., The ratio of total ammonium and sodium to total sulfate). Then, the appropriate set of equilibrium and mass and charge conservation relationships are solved to calculate the phase state and equilibrium concentrations (Table 1). Each of ten subcases has its own solution procedure and a distinct set of possible species at equilibrium.

### 3 Development of HDDM-3D/PM

HDDM-3D/PM directly computes the high-order DDM sensitivity coefficients of PM concentrations to input parameters, such as emissions, initial and boundary conditions by solving derivatives of the original equilibrium and conservation equations. First- and second-order sensitivity coefficients are defined as

$$S_{ij}^{(1)} = \frac{\partial C_i}{\partial p_j} \quad (4)$$

$$S_{ijk}^{(2)} = \frac{\partial^2 C_i}{\partial p_j \partial p_k} \quad (5)$$

where  $S_{ijk}^{(2)}$  denotes second-order sensitivity of species  $i$  to parameters  $j$  and  $k$ ;  $C_i$  denotes the ambient concentration of species  $i$ ; and  $p_j$  and  $p_k$  denote any two input parameters of interest. HDDM-3D/PM calculates semi-normalized sensitivity coefficients, expressed in the same units as concentration and allows for easier interpretation and application:

$$S_{ij}^{(1)} = \frac{\partial C_i}{\partial \varepsilon_j} \quad (6)$$

$$S_{ijk}^{(2)} = \frac{\partial^2 C_i}{\partial \varepsilon_j \partial \varepsilon_k} \quad (7)$$

where  $\varepsilon_j$  and  $\varepsilon_k$  are relative perturbations in parameters  $p_j$  and  $p_k$ , and they are related to the absolute perturbation of a parameter by  $\delta \varepsilon = \frac{\delta p}{p}$ .

The fundamental steps to obtain high-order DDM-3D sensitivities for PM from CMAQ are similar to those for the gaseous species. Taking second-order derivatives of the

## GMDD

4, 2605–2633, 2011

### Development of the high-order decoupled direct method

W. Zhang et al.

Title Page

Abstract

Introduction

Conclusions

References

Tables

Figures

◀

▶

◀

▶

Back

Close

Full Screen / Esc

Printer-friendly Version

Interactive Discussion



governing equation results in a similar equation which can be solved for second-order sensitivity of PM:

$$\frac{\partial S_{ijk}^{(2)}}{\partial t} = -\nabla(\mathbf{u}S_{ijk}^{(2)}) + \nabla(\mathbf{K}\nabla S_{ijk}^{(2)}) + \mathbf{J}_i \mathbf{S}_{jk}^{(2)} + f(C_i, S_{ij}^{(1)}, S_{ik}^{(1)}, \mathbf{u}, \mathbf{K}, R_i, E_i) \quad (8)$$

$S_{ijk}^{(2)}$  is the second-order sensitivity of species  $i$  with respect to parameters  $p_j$  and  $p_k$ ;  $S_{ij}^{(1)}$  and  $S_{ik}^{(1)}$  are first-order sensitivities of species  $i$  to parameters  $p_j$  and  $p_k$ , respectively;  $\mathbf{J}_i$  is the  $i$ -th row of Jacobian matrix defined as  $J_{ik} = \partial R_{ik} / \partial C_k$ .  $k$  is the  $k$ -th species in the concentration vector.  $\mathbf{S}_{jk}^{(2)}$  is the vector of second-order sensitivity coefficients.  $f$  is basically a function primarily of  $C_i$ ,  $S_{ij}^{(1)}$ , and  $S_{ik}^{(1)}$ . It can also be related to  $\mathbf{u}$ ,  $\mathbf{K}$ ,  $R_i$ , and  $E_i$ , depending on the types of sensitivity parameters. Details of  $f$  can be found in Eq. (9) in Hakami et al. (2003).

The majority of the processes in the aerosol module are linear, allowing for direct propagation of sensitivity coefficients using Eq. (8). However, the algorithmic treatment of secondary inorganic aerosol interactions with surrounding gases (i.e.,  $\text{SO}_2$ ,  $\text{NH}_3$ ,  $\text{HNO}_3$ , and  $\text{HCl}$ ) precludes direct application of Eq. (8); therefore, a different treatment for inorganic aerosol species in ISORROPIA is necessary to implement HDDM-3D/PM.

The implementation of HDDM in ISORROPIA involves differentiation of the equilibrium reactions that are involved in determining the concentrations of each species. For example, the equilibrium reaction for the balance between nitric acid gas ( $\text{HNO}_{3(g)}$ ) and nitrate ion ( $\text{NO}_3^-$ ) is



The corresponding equilibrium expression is

$$K = \frac{[\text{H}^+][\text{NO}_3^-] \gamma_{\text{HNO}_3}^2}{[\text{HNO}_3][\text{H}_2\text{O}]^2 RT} \quad (10)$$

Development of the high-order decoupled direct method

W. Zhang et al.

Title Page

Abstract

Introduction

Conclusions

References

Tables

Figures

⏪

⏩

◀

▶

Back

Close

Full Screen / Esc

Printer-friendly Version

Interactive Discussion





where  $K$  is the equilibrium constant;  $[A]$  denotes the molar concentration of  $A$ ;  $\gamma_{\text{HNO}_3}$  is the mean activity coefficient of  $\text{H}^+$  and  $\text{NO}_3^-$ ;  $R$  is the universal gas constant; and  $T$  is temperature. Taking the logarithmic derivative of Eq. (10) with respect to the first parameter of interest ( $\rho_1$ , where for brevity,  $T$  is assumed constant) leads to the expression of first-order sensitivity equation:

$$\frac{S_{\text{H}^+, \rho_1}^{(1)}}{[\text{H}^+]} + \frac{S_{\text{NO}_3^-, \rho_1}^{(1)}}{[\text{NO}_3^-]} - \frac{S_{\text{HNO}_3, \rho_1}^{(1)}}{[\text{HNO}_3]} + \frac{2S_{\gamma_{\text{HNO}_3}, \rho_1}^{(1)}}{\gamma_{\text{HNO}_3}} - \frac{2S_{\text{H}_2\text{O}, \rho_1}^{(1)}}{[\text{H}_2\text{O}]} = 0 \quad (11)$$

Differentiating Eq. (11) with respect to the second parameter of interest ( $\rho_2$ ) gives the equation for second-order sensitivity:

$$\begin{aligned} & \frac{S_{\text{H}^+, \rho_1, \rho_2}^{(2)}}{[\text{H}^+]} + \frac{S_{\text{NO}_3^-, \rho_1, \rho_2}^{(2)}}{[\text{NO}_3^-]} - \frac{S_{\text{HNO}_3, \rho_1, \rho_2}^{(2)}}{[\text{HNO}_3]} + \frac{2S_{\gamma_{\text{HNO}_3}, \rho_1, \rho_2}^{(2)}}{\gamma_{\text{HNO}_3}} - \frac{2S_{\text{H}_2\text{O}, \rho_1, \rho_2}^{(2)}}{[\text{H}_2\text{O}]} \\ & = \frac{S_{\text{H}^+, \rho_1}^{(1)} S_{\text{H}^+, \rho_2}^{(1)}}{[\text{H}^+]^2} + \frac{S_{\text{NO}_3^-, \rho_1}^{(1)} S_{\text{NO}_3^-, \rho_2}^{(1)}}{[\text{NO}_3^-]^2} - \frac{S_{\text{HNO}_3, \rho_1}^{(1)} S_{\text{HNO}_3, \rho_2}^{(1)}}{[\text{HNO}_3]^2} + \frac{2S_{\gamma_{\text{HNO}_3}, \rho_1}^{(1)} S_{\gamma_{\text{HNO}_3}, \rho_2}^{(1)}}{\gamma_{\text{HNO}_3}^2} - \frac{2S_{\text{H}_2\text{O}, \rho_1}^{(1)} S_{\text{H}_2\text{O}, \rho_2}^{(1)}}{[\text{H}_2\text{O}]^2} \end{aligned} \quad (12)$$

Repeating the same process with the other equilibrium reactions involved in the system gives similar expressions to Eq. (12). Combining them with mass and charge balance equations leads to a system of linear equations (Table 1) with which second-order sensitivities can be calculated. Calculating second-order DDM-3D sensitivities depends on the corresponding first-order sensitivities, so second-order sensitivities are computed sequentially following the first-order sensitivities in the same model run. Typically, the corresponding first-order sensitivities are always desired. Comparing Eqs. (11) and (12), identical coefficient terms multiplying the sensitivities are found on the left-hand sides, which reduces computational cost by allowing the two systems of linear equations to share the same coefficient matrix. Overall, the computational cost of second-order sensitivities is very close to that of first-order because the main computing processes (mainly transport) are the same for each sensitivity.

Development of the high-order decoupled direct method

W. Zhang et al.

Title Page

Abstract

Introduction

Conclusions

References

Tables

Figures



Back

Close

Full Screen / Esc

Printer-friendly Version

Interactive Discussion



In ISORROPIA, the mean activity coefficients are determined by Bromley's formula (Bromley, 1973). Sensitivities of the mean activity coefficients,  $S_{\log Y_{\text{HNO}_3}, P_1}^{(1)}$  and  $S_{\log Y_{\text{HNO}_3}}^{(2)}$  in Eqs. (11) and (12), are calculated by directly differentiating Bromley's formulas. As the activity coefficients are functions of the ion concentrations, their sensitivities are finally expressed as the combinations of sensitivities of relevant ion concentrations.

The liquid water content of aerosols is computed by the Zdanovskii-Stokes-Robinson (ZSR) relationship (Stokes and Robinson, 1966):

$$[\text{H}_2\text{O}] = \sum_i \frac{E_i}{m_{0i}} \quad (13)$$

where  $E_i$  is concentration of the  $i$ -th electrolyte in the multicomponent solution;  $m_{0i}$  is the molality of a solution with only the  $i$ -th electrolyte and the same water activity as the multicomponent solution. Sensitivities of the liquid water content are obtained by differentiating Eq. (13). Because the concentrations of electrolytes are calculated from the equilibrium ion concentrations, both first- and second-order sensitivities of liquid water content can be ultimately expressed as a function of ion sensitivities:

$$S_{\text{H}_2\text{O}}^{(1)} = \sum_i \frac{1}{m_{0i}} \sum_j \frac{\partial E_i}{\partial A_j} S_{A_j}^{(1)} \quad (14)$$

$$S_{\text{H}_2\text{O}}^{(2)} = \sum_i \frac{1}{m_{0i}} \sum_j \frac{\partial E_i}{\partial A_j} S_{A_j}^{(2)} \quad (15)$$

where  $A_j$  represents the  $j$ -th ionic species in the system.

ISORROPIA uses different algorithms to treat neutralized and acidic aerosol, so this work applied a case-specific approach when implementing HDDM-3D sensitivity analysis. Depending on the acidity of the aerosol, each subcase has its own solution routine and assumptions. For example, the neutralized aerosol algorithm assumes that bisulfate ions are minor species, and its concentration is adjusted after solving the equilibrium reactions of nitrate, nitric acid gas, ammonium, and ammonia gas. Alternatively, the acidic algorithm assumes that either ammonia or nitric acid gas is a minor

**Development of the high-order decoupled direct method**

W. Zhang et al.

Title Page

Abstract

Introduction

Conclusions

References

Tables

Figures

⏪

⏩

◀

▶

Back

Close

Full Screen / Esc

Printer-friendly Version

Interactive Discussion



species and resolves its final concentration after determining aerosol concentrations of their counterparts. This feature was usually neglected in previous implementations of DDM in ISORROPIA, which caused discrepancies between BF and DDM sensitivities. The problem is now solved by the case-specific approach, which exactly follows the treatment of ISORROPIA for different aerosols during HDDM implementation.

## 4 Results and discussion

The performance of HDDM-3D/PM is evaluated in both the stand-alone ISORROPIA and the CMAQ model for inorganic species. In the stand-alone ISORROPIA, the HDDM-3D/PM sensitivities were compared to brute-force sensitivities (first- and second- order) calculated by Eqs. (1) and (2), using a relative perturbation of 1%. The input concentrations of total sulfate, ammonium, and nitrate range from 0.1 to 10  $\mu\text{mol m}^{-3}$  with an incremental of 0.1  $\mu\text{mol m}^{-3}$ . The input concentrations of total sodium and chloride are 0.5 and 1  $\mu\text{mol m}^{-3}$ , respectively (Table 2). These inputs are consistent with the typical chemical composition of inorganic aerosols (Nenes et al., 1998b) and are also over a wide range allowing each subcase in ISORROPIA to be tested. The inorganic aerosol species are assumed to be in metastable state in CMAQ4.5, so the aerosols with the same chemical composition but different relative humidities are treated using the same algorithm. Therefore, we used a fixed relative humidity of 95 % for stand-alone testing.

We first compared the first-order DDM-3D and BF sensitivities of the five major ions (i.e.,  $\text{H}^+$ ,  $\text{NH}_4^+$ ,  $\text{SO}_4^{2-}$ ,  $\text{HSO}_4^-$ ,  $\text{NO}_3^-$ ) with respect to input total concentrations of sulfate, ammonium, and nitrate (Fig. 1). Good agreement is found between first-order BF and DDM sensitivities for all species (slope = 1 and  $R^2 = 0.99$ ), which is essential for evaluating the second-order sensitivities due to the dependence of second-order DDM-3D and BF sensitivities on the first-order counterparts.

The same comparison was conducted for second-order BF and DDM-3D sensitivities (Fig. 2). Although most of the points fall on the one-to-one line (slope = 1,  $R^2 = 0.95$ ),

## Development of the high-order decoupled direct method

W. Zhang et al.

Title Page

Abstract

Introduction

Conclusions

References

Tables

Figures



Back

Close

Full Screen / Esc

Printer-friendly Version

Interactive Discussion



discrepancies were found for some second-order sensitivities (Fig. 2). This is due to the noisy behavior of BF. As mentioned above, as the order of sensitivity coefficients increases, the two types of errors of BF approximations can become significantly larger. In other words, a lower degree of agreement between DDM-3D and BF are expected for second-order sensitivities. Our investigation into the noisy behavior of second-order BF sensitivities shows that second-order BF sensitivities vary dramatically with various sizes of perturbation ( $\Delta\rho$ ) and the convergence criteria of the ISORROPIA solution algorithm ( $\Delta\eta$ ) (Fig. 3). Further investigation into the charge balance for second-order BF and DDM-3D sensitivities revealed that the charge balance for BF sensitivities is not satisfied when they exhibit a noisy behavior. On the other hand, the charge balance is satisfied for DDM-3D sensitivities. These results strongly suggest that the HDDM-3D sensitivity coefficients are much more stable, while the BF second-order sensitivity coefficients are subject to significant numerical noise.

HDDM-3D/PM is applied to simulate a winter episode: 1–7 January 2004. Winter episodes have higher nitrate levels, which is a more stringent test of HDDM-3D/PM. The modeling domain covers the entire continental United States and portions of Canada and Mexico (Fig. 4) using a 36-km horizontal grid-spacing and thirteen vertical layers extending about 16 km above the ground. The meteorological fields were developed using the Fifth-Generation PSU/NCAR Mesoscale Model (MM5) (Grel et al., 1994). Emissions were prepared using the Sparse Matrix Operator Kernel Emissions (SMOKE) model (CEP, 2003). SAPRC99\_AE4\_AQ was selected as the chemical mechanism (Carter, 2000; Binkowski and Roseelle, 2003).

The sensitivities of aerosol sulfate, nitrate, and ammonium to domain-wide  $\text{SO}_2$ ,  $\text{NO}_x$ , and  $\text{NH}_3$  emissions are studied in this simulation. During a single simulation, HDDM-3D/PM provides all the sensitivities of interest for each grid at each time step. The spatial patterns of first- and second-order DDM sensitivities of aerosol sulfate to  $\text{SO}_2$  show that the most sensitive area is the Eastern US (Fig. 4); since this region is the area with the highest  $\text{SO}_2$  emissions, these sensitivities were expected. Spatial distributions of first- and second-order sensitivities are found to be consistent. The

**Development of the high-order decoupled direct method**

W. Zhang et al.

[Title Page](#)[Abstract](#)[Introduction](#)[Conclusions](#)[References](#)[Tables](#)[Figures](#)[Back](#)[Close](#)[Full Screen / Esc](#)[Printer-friendly Version](#)[Interactive Discussion](#)

magnitudes of the second-order sensitivities are smaller, and usually opposite in sign, but still indicate a significant contribution to the total response.

Comparison of first- and second-order BF and HDDM-3D/PM sensitivities of sulfate, nitrate, ammonium, and  $PM_{2.5}$  to domain-wide  $SO_2$ ,  $NO_x$ , and  $NH_3$  emissions find similar results to the stand-alone version (Figs. 5 and 6). First- and second-order BF sensitivities are calculated using Eqs. (1) and (2) with a 50 % reduction of each emission of interest, respectively. A choice of 50 % is made to minimize the impact of noise for BF sensitivities when taking a small difference between two relatively large concentrations though it is expected that nonlinearities may be of some importance over this range. Using a smaller reduction (say 10 %) leads to considerably larger error, which has been identified when testing HDDM-3D/PM in the stand-alone ISORROPIA. Most of the DDM-3D and BF first-order sensitivities are in good agreement with an overall slope of 0.9 and  $R^2$  of 0.91 (Fig. 5). The degree of agreement between DDM-3D and BF sensitivities of  $PM_{2.5}$  to  $NO_x$  and  $NH_3$  emissions is improved from  $R^2 = 0.63$  to  $R^2 = 0.93$  by the case-specific DDM approach in ISORROPIA. Sensitivity of aerosol nitrate to  $SO_2$  emissions is of concern to policy makers since the nitrate levels may be increased from  $SO_2$  emission controls (West et al., 1999). A relatively low degree of agreement was found between DDM-3D and BF sensitivities of nitrate to  $SO_2$  (Fig. 5c). However, nitrate concentrations are usually expected to increase with decreasing  $SO_2$  emissions, so the first-order sensitivity should be negative, as is shown by DDM-3D. The BF, however, is producing a significant amount of positive sensitivities, which is due to the nonlinear dependence of nitrate on  $SO_2$  emissions coupled with numerical noise. The comparison for sensitivity of sulfate to  $NO_x$  has two branches that are slightly off the one-to-one line. These disagreements are caused by cloud processes as additional testing shows that the discrepancies disappear when the cloud module is turned off. The disagreement for the sensitivity of sulfate to  $NH_3$  also comes from the cloud module where  $SO_2$  is oxidized to sulfate. The oxidation process is highly affected by the pH value, and the response of sulfate to  $NH_3$  is quite nonlinear. BF sensitivities of sulfate to  $NH_3$  are strongly affected by this nonlinearity. Further

## GMDD

4, 2605–2633, 2011

### Development of the high-order decoupled direct method

W. Zhang et al.

Title Page

Abstract

Introduction

Conclusions

References

Tables

Figures



Back

Close

Full Screen / Esc

Printer-friendly Version

Interactive Discussion



investigation showed that they change dramatically with the perturbation sizes as well as the BF approaches (i.e., forward and central finite difference). Overall, first-order BF and DDM-3D sensitivities compared well. BF sensitivities become less accurate when the system is quite nonlinear. This also implies the significance of the nonlinear response and the necessity of performing high-order sensitivity analysis.

Second-order DDM-3D sensitivities are also evaluated using BF. Good agreement is found for  $S_{\text{SO}_4^-, \text{SO}_2, \text{SO}_2}^{(2)}$ ,  $S_{\text{SO}_4^-, \text{NO}_x, \text{NO}_x}^{(2)}$ ,  $S_{\text{NH}_4^+, \text{NO}_x, \text{NO}_x}^{(2)}$ , and  $S_{\text{NO}_3^-, \text{NO}_x, \text{NO}_x}^{(2)}$  (Fig. 6a, e, f, and g) while the correlations are relatively low for some sensitivities, such as  $S_{\text{NO}_3^-, \text{SO}_2, \text{SO}_2}^{(2)}$

and  $S_{\text{SO}_4^-, \text{NH}_3, \text{NH}_3}^{(2)}$  (Figs. 6c and i). As mentioned above, second-order BF sensitivities for stand-alone ISORROPIA are strongly affected by the size of the perturbation. Here, we also investigated the impact of perturbation size to second-order BF sensitivities. For each second-order sensitivity of interest, we compared the BF results with 10% and 50% emission reduction. The noisy behavior of second-order BF sensitivities is evident (Fig. 7). The two BF scenarios in particular show little consistency for second-order sensitivity of sulfate to  $\text{NH}_3$ , which suggests that BF is not an accurate way to describe the nonlinear response of sulfate to  $\text{NH}_3$  (Fig. 7g). The plot for second-order sensitivity of nitrate to  $\text{SO}_2$  also shows that the BF results vary significantly (Fig. 7c). Thus, BF is not able to accurately approximate second-order local sensitivities of PM in CMAQ. Given the good performance of HDDM in the stand-alone ISORROPIA, and the great scatter between implementing BF with different perturbations, the direct approach is expected to provide more reliable results.

The average computational cost of calculating one second-order sensitivity of PM is found to be very close to that of one first-order sensitivity. For one day simulation, the average model time needed by the aerosol module for one first-order and one second-order sensitivities are 9 and 11 min, respectively, given that the second-order sensitivity calculation uses the same solution algorithm as first-order sensitivity. Therefore, the time required by matrix factorization and transport-related computations is almost the same for first- and second-order sensitivities. An indirect cost associated

## Development of the high-order decoupled direct method

W. Zhang et al.

Title Page

Abstract

Introduction

Conclusions

References

Tables

Figures

◀

▶

◀

▶

Back

Close

Full Screen / Esc

Printer-friendly Version

Interactive Discussion



with the second-order sensitivity calculation is that all relevant first-order sensitivities should also be calculated, which is generally of interest anyway in any application involving high-order sensitivity (Hakami et al., 2003). On the other hand, BF needs more than one simulation, and its computational cost increases directly with the order and the number of sensitivity parameters. HDDM-3D/PM provides an efficient approach to conduct high-order sensitivity analysis as it computes high-order sensitivities at a similar computational effort as first-order sensitivities.

HDDM-3D/PM has many practical applications, most of which are based on Taylor series expansion (Hakami et al., 2003):

$$C(\Delta\varepsilon) = C(0) + \Delta\varepsilon S^{(1)}(0) + \frac{\Delta\varepsilon^2}{2} S^{(2)}(0) + \text{higher order terms} \quad (16)$$

where  $C(0)$  stands for the pollutant concentration at base case emissions and  $C(\Delta\varepsilon)$  with a perturbation of  $\Delta\varepsilon$  in emissions. With Eq. (16), one can quickly compute the impact of emission perturbations on the ambient concentrations of pollutants. Including the second-order term (i.e., the third term on the right hand side of Eq. 16) is expected to reduce the error between the approximations using Taylor series expansion and the model simulation. For example, assuming 50% of domain-wide  $\text{NO}_x$  emissions are reduced in the simulation above, we predicted the concentration of nitrate using first- and second-order Taylor series expansion (Eq. 16) and compared them with model simulation (Fig. 8). Predictions using second-order Taylor series expansions are closer to the model simulation than those using first-order Taylor series expansions (Fig. 8). Thus, including the second-order term in Taylor series approximation improves the accuracy of prediction. This example also shows the importance of conducting high-order sensitivity analysis in a nonlinear system.

HDDM-3D/PM can be applied to source apportionment. The zero-out source contribution (ZOC) (i.e., the magnitude of the reduction in concentrations that would occur if the sources of interest did not exist) can be calculated by Eq. (16) with  $\Delta\varepsilon = -1$  (Cohan et al., 2005). Consider two emission sources ( $p_j$  and  $p_k$ ) that are perturbed simultaneously. The expression of ZOC of species  $i$  ( $\text{ZOC}_i$ ) can be obtained from Eq. (16) with

Development of the high-order decoupled direct method

W. Zhang et al.

Title Page

Abstract

Introduction

Conclusions

References

Tables

Figures



Back

Close

Full Screen / Esc

Printer-friendly Version

Interactive Discussion



multiple sensitivity parameters:

$$\text{ZOC}_i(p_j, p_k) \approx (S_{i,j}^{(1)} - 0.5S_{i,j,j}^{(2)}) + (S_{i,k}^{(1)} - 0.5S_{i,k,k}^{(2)}) - S_{i,j,k}^{(2)} \quad (17)$$

This approach is able to apportion secondary PM species to their precursor gases based on chemical and physical processes. The last term in Eq. (17) is the cross sensitivity, which represents the interactions between the two emissions. HDDM-3D/PM can also be applied to conduct control strategy optimization, uncertainty analysis of air quality modeling, and emission inventory assessment based on Eq. (16). Those applications are currently limited to gaseous species, such as ozone (Cohan et al., 2006; Tian et al., 2010). The development of HDDM-3D/PM now makes these applications possible for PM species.

*Acknowledgements.* This research was made possible by funding from Conoco-Phillips Inc. and US EPA (Grant numbers: RD83215910, RD83362601, RD83096001, RD82897602, and RD83107601).

*Disclaimer.* The contents of this publication are solely the responsibility of the grantee and do not necessarily represent the official views of the US EPA. Further, US EPA does not endorse the purchase of any commercial products or services mentioned in the publication.

## References

- Ansari, A. S. and Pandis, S. N.: Response of inorganic PM to precursor concentrations, *Environ. Sci. Technol.*, 32, 2706–2714, 1998.
- Bergin, M. S., Russell, A. G., Odman, M. T., Cohan, D. S., and Chameldes, W. L.: Single-Source Impact Analysis Using Three-Dimensional Air Quality Models, *J. Air Waste Manage.*, 58, 1351–1359, 2008.
- Binkowski, F. S. and Roselle, S. J.: Models-3 community multiscale air quality (CMAQ) model aerosol component – 1. Model description, *J. Geophys. Res.-Atmos.*, 108, 4183, doi:10.1029/2001JD001409, 2003.

# GMDD

4, 2605–2633, 2011

## Development of the high-order decoupled direct method

W. Zhang et al.

Title Page

Abstract

Introduction

Conclusions

References

Tables

Figures

⏪

⏩

◀

▶

Back

Close

Full Screen / Esc

Printer-friendly Version

Interactive Discussion





---

**Development of the  
high-order decoupled  
direct method**W. Zhang et al.

---

[Title Page](#)[Abstract](#)[Introduction](#)[Conclusions](#)[References](#)[Tables](#)[Figures](#)[⏪](#)[⏩](#)[◀](#)[▶](#)[Back](#)[Close](#)[Full Screen / Esc](#)[Printer-friendly Version](#)[Interactive Discussion](#)

- Bromley, L. A.: Thermodynamic properties of strong electrolytes in aqueous solutions, *Aiche J.*, 19, 313–320, 1973.
- Byun, D. and Schere, K. L.: Review of the Governing Equations, Computational Algorithms, and Other Components of the Models-3 Community Multiscale Air Quality (CMAQ) Modeling System, *Appl. Mech. Rev.*, 59, 51–77, 2006.
- 5 Carter, W. P. L.: Documentation of the SAPRC99 chemical mechanism for VOC and reactivity assessment, Air Pollution Research Center and College of Engineering, Center for Environmental Research and Technology, University of California, Riverside, CA, 2000.
- CEP: Sparse Matrix Operator Kernel Emissions Modeling System (SMOKE) User manual; Carolina Environmental Program, 2003.
- 10 Cohan, D. S., Hakami, A., Hu, Y. T., and Russell, A. G.: Nonlinear response of ozone to emissions: Source apportionment and sensitivity analysis, *Environ. Sci. Technol.*, 39, 6739–6748, 2005.
- Cohan, D. S., Tian, D., Hu, Y. T., and Russell, A. G.: Control strategy optimization for attainment and exposure mitigation: Case study for ozone in Macon, Georgia, *Environ. Manage.*, 38, 451–462, 2006.
- 15 Cohan, D. S., Koo, B., and Yarwood, G.: Influence of uncertain reaction rates on ozone sensitivity to emissions, *Atmos. Environ.*, 44, 3101–3109, 2010.
- Dunker, A. M.: The Decoupled Direct Method For Calculating Sensitivity Coefficients in Chemical Kinetics, *J. Chem. Phys.*, 81, 2385–2393, 1984.
- 20 ENVIRON: Users' Guide, Comprehensive Air Quality Model with Extensions (CAMx), Version 4.20; ENVIRON International Corporation, 2005.
- Fountoukis, C. and Nenes, A.: ISORROPIA II: a computationally efficient thermodynamic equilibrium model for  $K^+$ - $Ca^{2+}$ - $Mg^{2+}$ - $NH_4^+$ - $Na^+$ - $SO_4^{2-}$ - $NO_3^-$ - $Cl^-$ - $H_2O$  aerosols, *Atmos. Chem. Phys.*, 7, 4639–4659, doi:10.5194/acp-7-4639-2007, 2007.
- 25 Galloway, T. S., Brown, R. J., Browne, M. A., Dissanayake, A., Lowe, D., Jones, M. B., and Depledge, M. H.: A multibiomarker approach to environmental assessment, *Environ. Sci. Technol.*, 38, 1723–1731, 2004.
- Grell, G., Dudhia, J., and Stauffer, D.: A description of the Fifth-Generation Penn State/NCAR Mesoscale Model (MM5), NCAR, NCAR/TN 398+STR, 1994.
- 30 Hakami, A., Odman, M. T., and Russell, A. G.: High-order, direct sensitivity analysis of multidimensional air quality models, *Environ. Sci. Technol.*, 37, 2442–2452, 2003.
- Hakami, A., Odman, M. T., and Russell, A. G.: Nonlinearity in atmospheric re-

## Development of the high-order decoupled direct method

W. Zhang et al.

[Title Page](#)

[Abstract](#)

[Introduction](#)

[Conclusions](#)

[References](#)

[Tables](#)

[Figures](#)

◀

▶

◀

▶

[Back](#)

[Close](#)

[Full Screen / Esc](#)

[Printer-friendly Version](#)

[Interactive Discussion](#)



sponse: A direct sensitivity analysis approach, *J. Geophys. Res.-Atmos.*, 109, D15303, doi:10.1029/2001JD004502, 2004.

Kaiser, J.: Mounting evidence indicts fine-particle pollution, *Science*, 307, 1858–1861, 2005.

Kelly, J. T., Bhawe, P. V., Nolte, C. G., Shankar, U., and Foley, K. M.: Simulating emission and chemical evolution of coarse sea-salt particles in the Community Multiscale Air Quality (CMAQ) model, *Geosci. Model Dev.*, 3, 257–273, doi:10.5194/gmd-3-257-2010, 2010.

Koo, B., Dunker, A. M., and Yarwood, G.: Implementing the decoupled direct method for sensitivity analysis in a particulate matter air quality model, *Environ. Sci. Technol.*, 41, 2847–2854, 2007.

Koo, B., Wilson, G., and Yarwood, G.: High-order Decoupled Direct Method (HDDM) Radical Output Improvements in the Comprehensive Air-quality Model with Extensions (CAMx), 582-7-84005-FY10-27, 2010.

Mendoza-Dominguez, A. and Russell, A. G.: Iterative inverse modeling and direct sensitivity analysis of a photochemical air duality model, *Environ. Sci. Technol.*, 34, 4974–4981, 2000.

Napelenok, S. L., Cohan, D. S., Hu, Y. T., and Russell, A. G.: Decoupled direct 3D sensitivity analysis for particulate matter (DDM-3D/PM), *Atmos. Environ.*, 40, 6112–6121, 2006.

Nenes, A., Pandis, S. N., and Pilinis, C.: ISORROPIA: A new thermodynamic equilibrium model for multiphase multicomponent inorganic aerosols, *Aqua. Geochem.*, 4, 123–152, 1998a.

Nenes, A., Pilinis, C., and Pandis, S. N.: Continued Development and Testing of a New Thermodynamic Aerosol Module for Urban and Regional Air Quality Models, *Atmos. Environ.*, 33, 1553–1560, 1998b.

Odman, M. T. and Ingram, C. L.: Multiscale Air Quality Simulation Platform (MAQSIP): Source code documentation and validation, Environmental Programs, North Carolina Supercomputing Center, Research Triangle Park, NC, 1996.

Odman, M. T., Boylan, J. W., Wilkinson, J. G., Russell, A. G., Mueller, S. F., Imhoff, R. E., Doty, K. G., Norris, W. B., and McNider, R. T.: Integrated modeling for air quality assessment: The Southern Appalachians mountains initiative project, *Journal De Physique Iv*, 12, 211–234, 2002.

Odum, J. R., Jungkamp, T. P. W., Griffin, R. J., Forstner, H. J. L., Flagan, R. C., and Seinfeld, J. H.: Aromatics, reformulated gasoline, and atmospheric organic aerosol formation, *Environ. Sci. Technol.*, 31, 1890–1897, 1997.

Schell, B., Ackermann, I. J., Hass, H., Binkowski, F. S., and Ebel, A.: Modeling the formation of secondary organic aerosol within a comprehensive air quality model system, *J. Geophys.*

---

**Development of the  
high-order decoupled  
direct method**


---

W. Zhang et al.

[Title Page](#)[Abstract](#)[Introduction](#)[Conclusions](#)[References](#)[Tables](#)[Figures](#)[Back](#)[Close](#)[Full Screen / Esc](#)[Printer-friendly Version](#)[Interactive Discussion](#)

Res.-Atmos., 106, 28275–28293, 2001.

Seinfeld, J. H. and Pandis, S. N.: Atmospheric Chemistry and Physics: From Air Pollution to Climate Change, 2nd Edn., Wiley, New York, 2006.

Stokes, R. H. and Robinson, R. A.: Interactions in aqueous nonelectrolyte solutions I: Solute-solvent equilibria, *J. Phys. Chem.-Us.*, 70, 2126–2131, 1966.

Tian, D., Cohan, D. S., Napelenok, S., Bergin, M., Hu, Y. T., Chang, M., and Russell, A. G.: Uncertainty Analysis of Ozone Formation and Response to Emission Controls Using Higher-Order Sensitivities, *J. Air Waste Manage.*, 60, 797–804, 2010.

US EPA: Air quality criteria for particulate matter, EPA/600/P-99/002aF, 2004.

Watson, J. G.: Visibility: Science and regulation, *J. Air Waste Manage.*, 52, 628–713, 2002.

West, J. J., Ansari, A. S., and Pandis, S. N.: Marginal PM<sub>2.5</sub>: Nonlinear aerosol mass response to sulfate reductions in the Eastern United States, *J. Air Waste Manage.*, 49, 1415–1424, 1999.

Yang, Y. J., Wilkinson, J. G., and Russell, A. G.: Fast, direct sensitivity analysis of multidimensional photochemical models, *Environ. Sci. Technol.*, 31, 2859–2868, 1997.

Zanobetti, A., Schwartz, J., and Dockery, D. W.: Airborne particles are a risk factor for hospital admissions for heart and lung disease, *Environ. Health Perspect.*, 108, 1071–1077, doi:10.2307/3434961, 2000.

**Development of the high-order decoupled direct method**

W. Zhang et al.

Title Page	
Abstract	Introduction
Conclusions	References
Tables	Figures
◀	▶
◀	▶
Back	Close
Full Screen / Esc	
Printer-friendly Version	
Interactive Discussion	

**Table 1.** Equilibrium Relations, Mass and Charge Balance of ISORROPIA.

Equilibrium Reactions	Equilibrium Constants
$\text{HSO}_4^- \leftrightarrow \text{H}^+ + \text{SO}_4^{2-}$	$K_1 = \frac{[\text{H}^+][\text{SO}_4^{2-}]\gamma_{\text{H}^+}\gamma_{\text{SO}_4^{2-}}}{[\text{HSO}_4^-]\gamma_{\text{HSO}_4^-}w_{\text{H}_2\text{O}}}$
$\text{NH}_3(\text{g}) + \text{H}_2\text{O}(\text{aq}) \leftrightarrow \text{NH}_4^+ + \text{OH}^-$	$K_2 = \frac{[\text{NH}_4^+][\text{OH}^-]\gamma_{\text{NH}_4^+}\gamma_{\text{OH}^-}}{P_{\text{NH}_3}a_w w_{\text{H}_2\text{O}}^2}$
$\text{HCl}(\text{g}) \leftrightarrow \text{H}^+ + \text{Cl}^-$	$K_3 = \frac{[\text{H}^+][\text{Cl}^-]\gamma_{\text{H}^+}\gamma_{\text{Cl}^-}}{P_{\text{HCl}}w_{\text{H}_2\text{O}}^2}$
$\text{HNO}_3(\text{g}) \leftrightarrow \text{H}^+ + \text{NO}_3^-$	$K_4 = \frac{[\text{H}^+][\text{NO}_3^-]\gamma_{\text{H}^+}\gamma_{\text{NO}_3^-}}{P_{\text{HNO}_3}w_{\text{H}_2\text{O}}^2}$
$\text{H}_2\text{O}(\text{aq}) \leftrightarrow \text{H}^+ + \text{OH}^-$	$K_w = \frac{[\text{H}^+][\text{OH}^-]\gamma_{\text{NH}_4^+}\gamma_{\text{OH}^-}}{a_w w_{\text{H}_2\text{O}}^2}$
$\text{Na}_2\text{SO}_4(\text{s}) \leftrightarrow 2\text{Na}^+ + \text{SO}_4^{2-}$	$K_5 = [\text{Na}^+]^2[\text{SO}_4^{2-}]\gamma_{\text{Na}^+}\gamma_{\text{SO}_4^{2-}}w_{\text{H}_2\text{O}}^{-3}$
$\text{NH}_4\text{Cl}(\text{s}) \leftrightarrow \text{NH}_3 + \text{HCl}$	$K_6 = P_{\text{NH}_3}P_{\text{HCl}}$
$(\text{NH}_4)_2\text{SO}_4(\text{s}) \leftrightarrow 2\text{NH}_4^+ + \text{SO}_4^{2-}$	$K_7 = [\text{NH}_4^+]^2[\text{SO}_4^{2-}]\gamma_{\text{NH}_4^+}^2\gamma_{\text{SO}_4^{2-}}w_{\text{H}_2\text{O}}^{-3}$
$\text{NaCl}(\text{s}) \leftrightarrow \text{Na}^+ + \text{Cl}^-$	$K_8 = [\text{Na}^+][\text{Cl}^-]\gamma_{\text{Na}^+}\gamma_{\text{Cl}^-}w_{\text{H}_2\text{O}}^{-2}$
$\text{NaNO}_3(\text{s}) \leftrightarrow \text{Na}^+ + \text{NO}_3^-$	$K_9 = [\text{Na}^+][\text{NO}_3^-]\gamma_{\text{Na}^+}\gamma_{\text{NO}_3^-}w_{\text{H}_2\text{O}}^{-2}$
$\text{NH}_4\text{NO}_3(\text{s}) \leftrightarrow \text{NH}_3(\text{g}) + \text{HNO}_3(\text{g})$	$K_{10} = P_{\text{NH}_3}P_{\text{HNO}_3}$
$\text{NaHSO}_4(\text{s}) \leftrightarrow \text{Na}^+ + \text{HSO}_4^{2-}$	$K_{11} = [\text{Na}^+][\text{HSO}_4^{2-}]\gamma_{\text{Na}^+}\gamma_{\text{HSO}_4^{2-}}w_{\text{H}_2\text{O}}^{-2}$
$\text{NH}_4\text{HSO}_4(\text{s}) \leftrightarrow \text{NH}_4^+ + \text{HSO}_4^-$	$K_{12} = [\text{NH}_4^+][\text{HSO}_4^-]\gamma_{\text{NH}_4^+}\gamma_{\text{HSO}_4^-}w_{\text{H}_2\text{O}}^{-2}$
$(\text{NH}_4)_3\text{H}(\text{SO}_4)_2(\text{s}) \leftrightarrow 3\text{NH}_4^+ + \text{HSO}_4^- + \text{SO}_4^{2-}$	$K_{13} = \frac{[\text{NH}_4^+]^3[\text{HSO}_4^-][\text{SO}_4^{2-}]\gamma_{\text{NH}_4^+}^3\gamma_{\text{HSO}_4^-}\gamma_{\text{SO}_4^{2-}}}{w_{\text{H}_2\text{O}}^5}$
<b>Mass Balance</b>	
$[t\text{Na}] = [\text{Na}^+] + 2[\text{Na}_2\text{SO}_4] + [\text{NaCl}] + [\text{NaNO}_3] + [\text{NaHSO}_4]$	
$[t\text{SO}_4] = [\text{SO}_4^{2-}] + [\text{HSO}_4^-] + [\text{Na}_2\text{SO}_4] + [\text{NaHSO}_4] + [(\text{NH}_4)_2\text{SO}_4] + [\text{NH}_4\text{HSO}_4] + 2[(\text{NH}_4)_3\text{H}(\text{SO}_4)_2]$	
$[t\text{NH}_4] = [\text{NH}_3] + [\text{NH}_4^+] + 2[(\text{NH}_4)_2\text{SO}_4] + [\text{NH}_4\text{HSO}_4] + 3[(\text{NH}_4)_3\text{H}(\text{SO}_4)_2] + [\text{NH}_4\text{Cl}] + [\text{NH}_4\text{NO}_3]$	
$[t\text{NO}_3] = [\text{HNO}_3] + [\text{NO}_3^-] + [\text{NaNO}_3] + [\text{NH}_4\text{NO}_3]$	
$[t\text{Cl}] = [\text{HCl}] + [\text{Cl}^-] + [\text{NaCl}] + [\text{NH}_4\text{Cl}]$	
<b>Charge Balance</b>	
$[\text{H}^+] + [\text{Na}^+] + [\text{NH}_4^+] = [\text{NO}_3^-] + [\text{Cl}^-] + 2[\text{SO}_4^{2-}] + [\text{HSO}_4^-] + [\text{OH}^-]$	

\* All quantities in [ ] denote molar concentrations, the unit is mol m<sup>-3</sup> air.



**Development of the  
high-order decoupled  
direct method**

W. Zhang et al.

[Title Page](#)[Abstract](#)[Introduction](#)[Conclusions](#)[References](#)[Tables](#)[Figures](#)[⏪](#)[⏩](#)[◀](#)[▶](#)[Back](#)[Close](#)[Full Screen / Esc](#)[Printer-friendly Version](#)[Interactive Discussion](#)**Table 2.** Input cases for testing of HDDM-PM using stand-alone ISORROPIA.

Parameters	Values ( $\mu\text{mol m}^{-3}$ )
Total Sulfate	0.1 ~ 10
Total Ammonium	0.1 ~ 10
Total Nitrate	0.1 ~ 10
Total Sodium	0.5
Total Chloride	1.0
Relative Humidity	95 %
Temperature	298 K

## Development of the high-order decoupled direct method

W. Zhang et al.

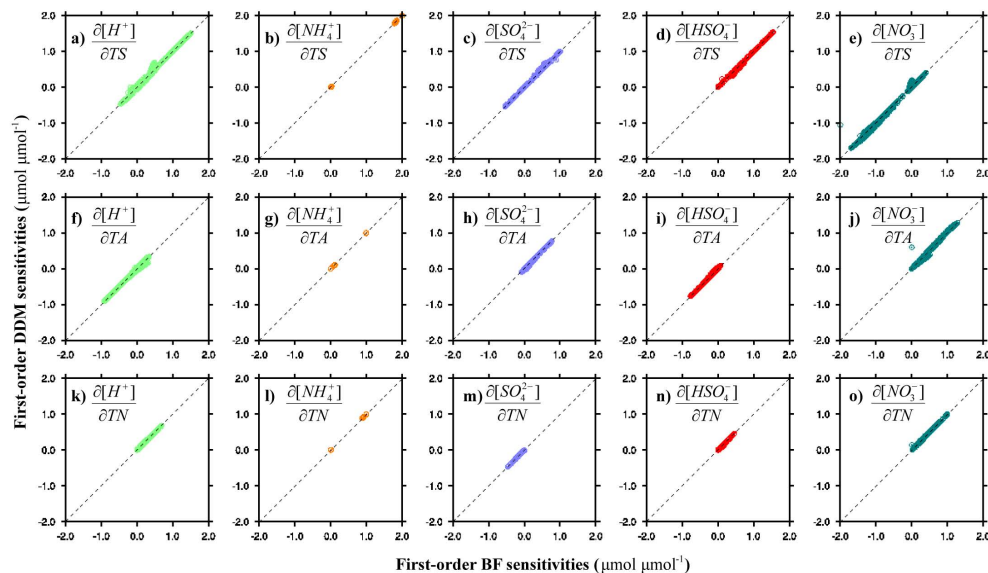


**Fig. 1.** Comparison of first-order DDM and BF sensitivity coefficients of the five major ions (i.e.,  $H^+$ ,  $NH_4^+$ ,  $SO_4^{2-}$ ,  $HSO_4^-$ , and  $NO_3^-$ ) to the change of total sulfate (TS), total ammonia (TA), and total nitrate (TN) in the stand-alone ISORROPIA. Each plot corresponds to the comparison of one sensitivity coefficient that is labeled on the upper left of the plot. For example, **(a)** shows the comparison of first-order sensitivity of hydrogen ion ( $H^+$ ) to total sulfate predicted by DDM and BF. The dashed line is the one-to-one line for reference of perfect agreement.

[Title Page](#)
[Abstract](#)
[Introduction](#)
[Conclusions](#)
[References](#)
[Tables](#)
[Figures](#)
[Back](#)
[Close](#)
[Full Screen / Esc](#)
[Printer-friendly Version](#)
[Interactive Discussion](#)


Development of the  
high-order decoupled  
direct method

W. Zhang et al.

Title Page

Abstract

Introduction

Conclusions

References

Tables

Figures



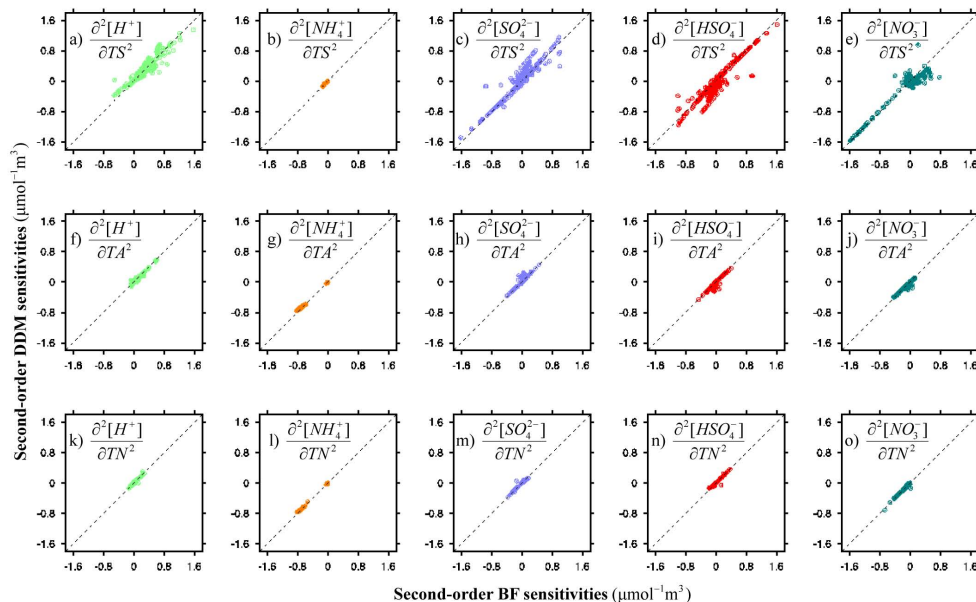
Back

Close

Full Screen / Esc

Printer-friendly Version

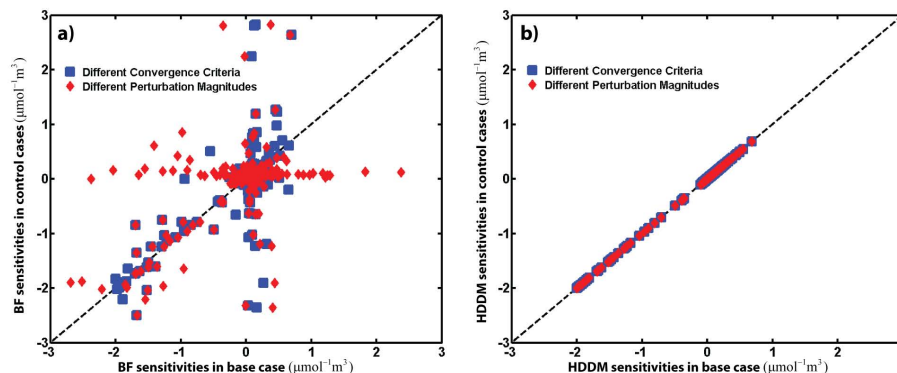
Interactive Discussion



**Fig. 2.** Comparison of second-order DDM and BF sensitivity coefficients of the five major ions (i.e.,  $H^+$ ,  $NH_4^+$ ,  $SO_4^{2-}$ ,  $HSO_4^-$ , and  $NO_3^-$ ) to the change of total sulfate (TS), total ammonia (TA), and total nitrate (TN) in the stand-alone ISORROPIA. Each plot corresponds to the comparison of one sensitivity coefficient that is labeled on the upper left of the plot. For example, **(a)** shows the comparison of second-order sensitivity of hydrogen ion ( $H^+$ ) to total sulfate predicted by DDM and BF. The dashed line is the one-to-one line for reference of perfect agreement.

## Development of the high-order decoupled direct method

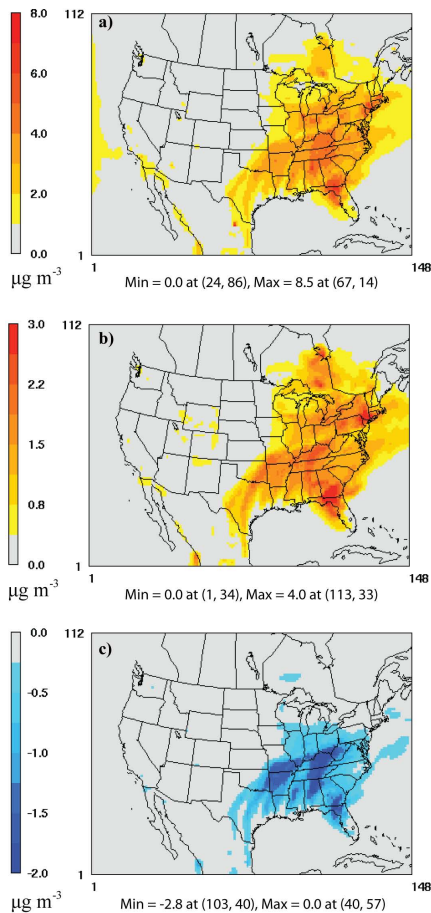
W. Zhang et al.



**Fig. 3.** Second-order sensitivity coefficients of aerosol nitrate to total sulfate in stand-alone ISORROPIA calculated by **(a)** BF and **(b)** HDDM under three conditions: (1) base case, where the perturbation used by BF ( $\Delta\rho$ ) = 1% and the convergence criteria of ISORROPIA ( $\Delta\eta$ ) =  $1 \times 10^{-10}$ ; (2) control case 1 (blue squares) with  $\Delta\rho$  = 1% and  $\Delta\eta$  =  $1 \times 10^{-3}$ ; and (3) control case 2 (red diamonds) with  $\Delta\rho$  = 0.1% and  $\Delta\eta$  =  $1 \times 10^{-10}$ . Results from the two control cases are compared to those from the base case. The dashed line is the one-to-one line.

[Title Page](#)
[Abstract](#)
[Introduction](#)
[Conclusions](#)
[References](#)
[Tables](#)
[Figures](#)
[⏪](#)
[⏩](#)
[◀](#)
[▶](#)
[Back](#)
[Close](#)
[Full Screen / Esc](#)
[Printer-friendly Version](#)
[Interactive Discussion](#)



**Fig. 4.** Spatial distribution of 24-h averages of **(a)** simulated concentration of sulfate, **(b)** first- and **(c)** second-order sensitivities of sulfate to  $\text{SO}_2$  at surface layer on 3 January 2004.

## Development of the high-order decoupled direct method

W. Zhang et al.

Title Page

Abstract

Introduction

Conclusions

References

Tables

Figures

◀

▶

◀

▶

Back

Close

Full Screen / Esc

Printer-friendly Version

Interactive Discussion



Development of the  
high-order decoupled  
direct method

W. Zhang et al.

Title Page

Abstract

Introduction

Conclusions

References

Tables

Figures

◀

▶

◀

▶

Back

Close

Full Screen / Esc

Printer-friendly Version

Interactive Discussion

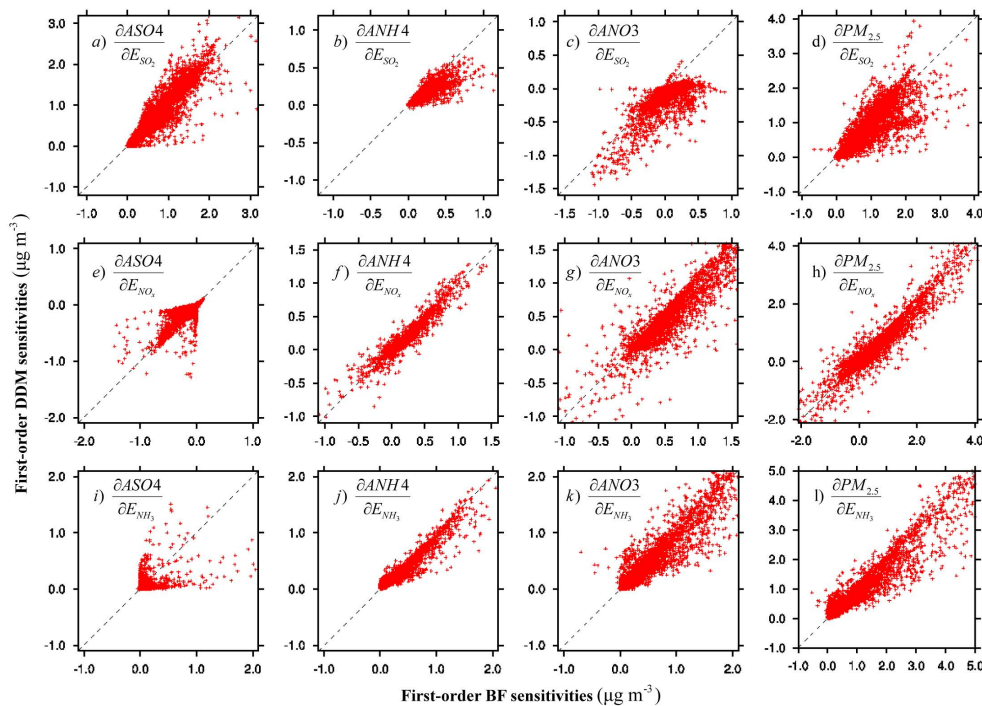


**Fig. 5.** Comparison of first-order sensitivities of sulfate, ammonium, nitrate, and  $PM_{2.5}$  to  $SO_2$ ,  $NO_x$ , and  $NH_3$  calculated by HDDM-3D/PM and BF at surface layer on 2 January 2004. ASO4, ANH4, and ANO3 denote aerosol sulfate, aerosol ammonium, and aerosol nitrate, respectively. Each plot represents one sensitivity coefficient that is labeled on the upper left of the plot. The dashed line is the one-to-one line.

## Development of the high-order decoupled direct method

W. Zhang et al.

Title Page

Abstract

Introduction

Conclusions

References

Tables

Figures

◀

▶

◀

▶

Back

Close

Full Screen / Esc

Printer-friendly Version

Interactive Discussion

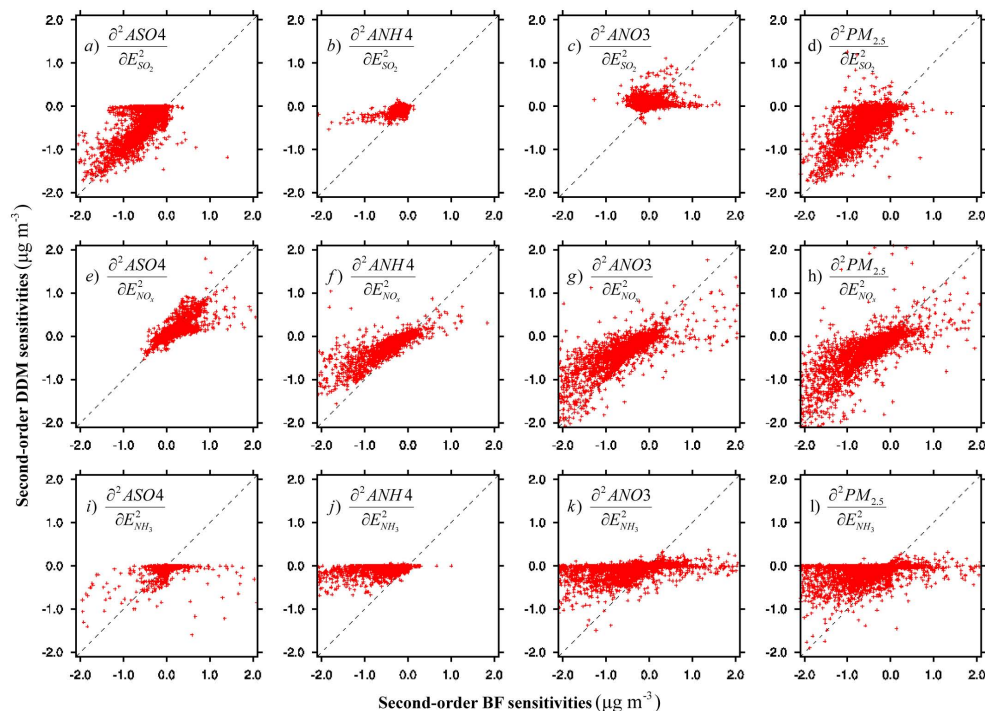


**Fig. 6.** Comparison of second-order sensitivities of sulfate, ammonium, nitrate, and  $PM_{2.5}$  to  $SO_2$ ,  $NO_x$ , and  $NH_3$  calculated by HDDM-3D/PM and BF at surface layer on 2 January 2004. ASO4, ANH4, and ANO3 denote aerosol sulfate, aerosol ammonium, and aerosol nitrate, respectively. Each plot represents one sensitivity coefficient that is labeled on the upper left of the plot. The dashed line is the one-to-one line indicating perfect agreement.

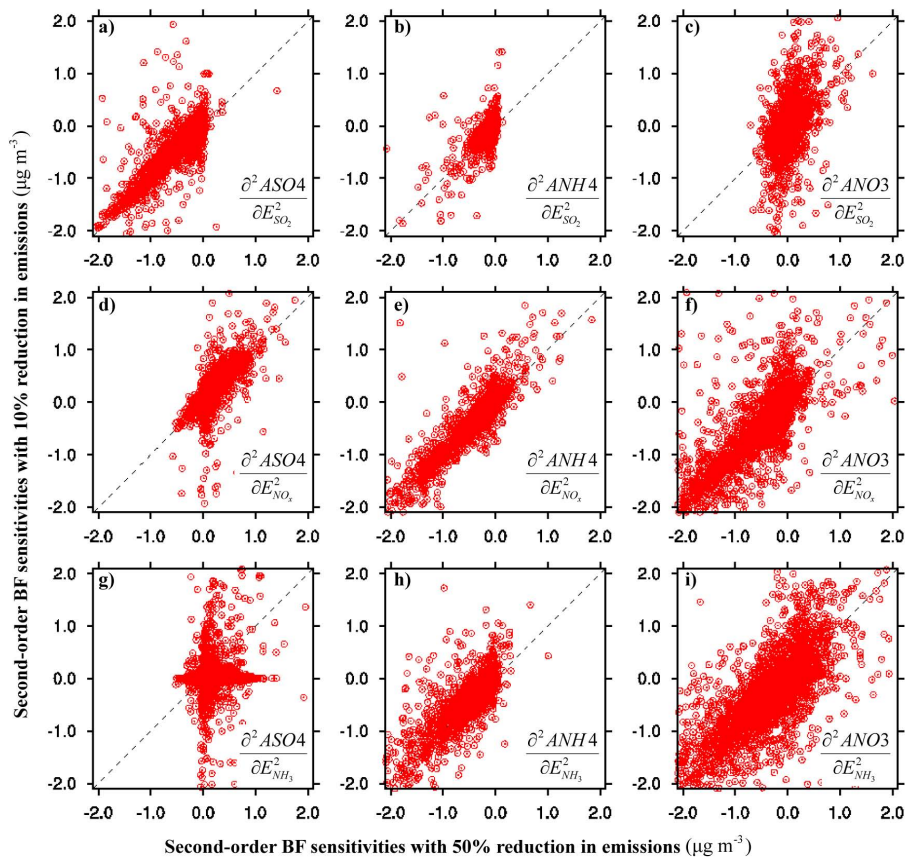


**Fig. 7.** Comparison of second-order BF sensitivities calculated with 10% and 50% perturbation in emissions using CMAQ simulation on 2 January 2004 at surface layer. ASO4, ANH4, and ANO3 denote aerosol sulfate, aerosol ammonium, and aerosol nitrate, respectively.

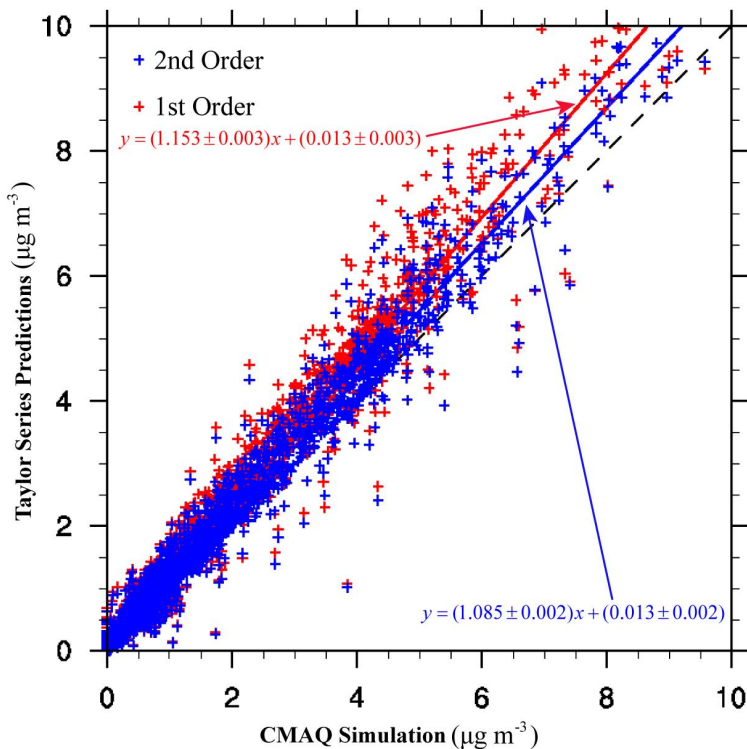


**Fig. 8.** Comparisons of model simulation concentrations of nitrate with a 50% reduction in  $\text{NO}_x$  and predictions using Taylor series expansion at 16:00 EDT on 2 January 2004. Red and blue points represent the predictions using first- and second-order Taylor expansion, respectively. Red and blue lines are the linear regression lines of first- and second-order Taylor series predictions to model simulation, respectively. The dashed line is the one-to-one line indicating perfect agreement.

**Development of the high-order decoupled direct method**

W. Zhang et al.

Title Page	
Abstract	Introduction
Conclusions	References
Tables	Figures
◀	▶
◀	▶
Back	Close
Full Screen / Esc	
Printer-friendly Version	
Interactive Discussion	

